



Contents lists available at SciVerse ScienceDirect

# Journal of Quantitative Spectroscopy & Radiative Transfer

journal homepage: [www.elsevier.com/locate/jqsrt](http://www.elsevier.com/locate/jqsrt)

## Corona discharge as a temperature probe of atmospheric air microwave plasma jet

Lenka Leštinská\*, Viktor Martišovitz, Zdenko Machala

Division of Environmental Physics, Faculty of Mathematics, Physics and Informatics, Comenius University, Mlynská dolina, Bratislava 842 48, Slovakia

### ARTICLE INFO

#### Article history:

Received 4 February 2011

Received in revised form

28 August 2011

Accepted 12 September 2011

Available online 16 September 2011

#### Keywords:

Microwave plasma jet

Corona

Optical emission spectroscopy

Temperature measurements

Thermocouple

### ABSTRACT

We developed and tested a new method for temperature measurements of near-LTE air plasmas at atmospheric pressure. This method is specifically suitable for plasmas at relatively low gas temperature (800–1700 K) with no appropriate radiation for direct spectroscopic temperature measurements. Corona discharge producing cold non-equilibrium plasma is employed as a source of excitation and is placed into the microwave plasma jet. The gas temperature of the microwave plasma jet is determined as the rotational temperature of  $N_2^*$  produced in the corona discharge. The corona probe temperature measurement was tested by the use of a thermocouple. We found a fairly good agreement between the two methods after correcting the thermocouple measured temperatures for radiative losses. The corona probe method can be generally applied to determine the temperature of the near-LTE plasmas and contrary to the thermocouple it can be used for higher plasma temperatures and is not affected by radiative losses and problems of interaction with the microwave plasma and electromagnetic fields.

© 2011 Elsevier Ltd. All rights reserved.

### 1. Introduction

Atmospheric pressure microwave (MW) or radio-frequency (RF) plasmas present considerable interest for various industrial or environmental applications such as surface treatment [1], carbon nanotube synthesis [2,3], trace element analysis [4], air pollution control, various biomedical applications [5,6], etc. The main advantage of MW plasmas is electrodeless operation, availability of cheap microwave sources at 2.45 GHz, good microwave to plasma energy coupling and no need of vacuum devices if operated at atmospheric pressure. MW or RF torches are sometimes used to preheat gases to high temperatures needed for other applications or for studying other discharge plasmas in preheated gases [7,8].

In general, it is very important to know the characteristics of the generated MW or RF plasma in order to ensure that it is suitable for a desired application. Optical emission spectroscopy (OES) is a good, reliable and non-intrusive method of plasma diagnostics. It enables identification of active species and radicals in the plasma, as well as temperature measurements (determination of vibrational and rotational and electronic excitation temperatures). At atmospheric pressure, rotational temperature equilibrates with the gas temperature owing to fast collisional relaxation [9,10]. In this paper we introduce a gas temperature diagnostic method for MW air plasma jets also applicable for other near equilibrium (near-LTE) plasma sources, or simply preheated gases.

### 2. Corona probe method

The gas temperature  $T_g$  in the plasma, one of the key plasma parameters, can be determined by OES by comparing measured and simulated atomic and molecular

\* Corresponding author.

E-mail address: [lenka.lestinska@fmph.uniba.sk](mailto:lenka.lestinska@fmph.uniba.sk) (L. Leštinská).

emission spectra of the generated plasma. This method is very convenient but sometimes overestimates the temperature if emission spectra of radicals are considered. The radicals or other species generated in the plasma can gain energy in the chemical processes of their production, which can contribute to the elevated temperature. This phenomenon was observed by several authors [9,10]. This implies that the best way to determine the plasma temperature by OES is to use the spectra of the particles that are present in the feeding gas. In air plasmas, the most convenient is to determine the gas temperature from  $N_2$  spectra, since  $N_2$  molecules are present in the feeding gas and are not produced by chemical processes in the plasma, like NO or OH radicals.

It is known that in discharges generated in air at atmospheric pressure, the emission of the first and second positive system of  $N_2$  is usually observed. In near-LTE MW plasma generated in air, however, the excitation of  $N_2$  takes place only at the temperatures above 6000 K [11]. Such high temperature is not reached in our plasma jet; therefore there is no  $N_2$  emission. Furthermore there is even no (or too weak to detect) emission of NO and OH radicals or  $O_2$  that are usually present in LTE air plasmas. With no appropriate radiation it is not possible to perform OES temperature diagnostics of the generated air plasma jet.

On the other hand, it is known that excited  $N_2$  is produced in non-equilibrium air plasmas, e.g. in the corona discharge. In this strongly non-equilibrium discharge,  $T_g$  is low (close to room temperature) but the high temperature of electrons is sufficient for the excitation of  $N_2$ . In the discharges at atmospheric pressure, the rotational temperature balances with the temperature of the surrounding gas  $T_g$ . So we put corona discharge directly into the MW plasma jet.  $N_2^*$  is then produced by electron-impact excitation but its rotational temperature equilibrates with the surrounding gas temperature—in our case, the temperature of the MW plasma jet. The cold corona discharge (when operated in ambient air,  $T_g=300 \pm 50$  K) does not significantly contribute to the increase of  $T_g$ . By using this corona probe, i.e. by combining the MW plasma with corona discharge, we can thus determine the temperature of MW plasma (as the rotational temperature of  $N_2^*$ ).

To test the reliability of this corona probe method, we also determined the temperature simultaneously by the thermocouple and the corona probe and compared the two measurements. A use of thermocouples to measure the temperature of the plasma generated at low pressures and high temperatures is affected by the heat transfer processes and the method is considered not very reliable in this case. At atmospheric pressure in general, thermocouples are being used for temperature measurements if the gas temperature and the gas flow rate are not too high. It is also suitable to use the thermocouple with the smallest probe diameter possible so that it does not affect the gas flows and the plasma itself. In some cases, the thermocouple is placed in a ceramic tube to prevent the heat losses along the thermocouple wires and also to support the thermocouple in a desired position. Plasma temperature was measured by a thermocouple for example in [12–14]. Nevertheless, since thermocouples are

based on measurements of small voltages ( $\sim$ mV), their performance may be affected by the presence of ionized gas. Therefore we consider temperatures obtained by thermocouples as estimative only.

### 3. Experimental setup

Litmas Red MW plasma torch powered by a 900 W magnetron, supplied from Richardson Electronics switching power generator SM1050, was used to generate atmospheric pressure air plasma with properties close to LTE. Microwaves generated by a magnetron are focused to the cylindrical plasma chamber made of a hardened teflon or  $Al_2O_3$ . A thin teflon tape is placed in the waveguide between the plasma chamber and magnetron to prevent the contamination of the magnetron or the resonant circulator by dust or gases which could cause its malfunction.

The MW discharge is ignited by pneumatic insertion of a metal igniter into the plasma chamber. The brush-shaped igniter (synchronized with the magnetron through the electronic unit) causes a local enhancement of the electric field resulting in a discharge ignition. The whole system is externally cooled with water and air. Contrary to the typical MW torch systems, in our case the gas is inserted downstream and tangentially through the two holes of the nozzle into the cylindrical plasma chamber. This is causing the swirl flow in the cylinder and generated swirling plasma is consequently blown out upstream through the central orifice of the nozzle. Experimental set-up and the basic torch characteristics are described in more detail in [15].

We use a special 75 mm long hollow stainless steel syringe needle with a diameter 0.9 mm supplied by DC high voltage of approximately 3.5 kV as a corona electrode. Corona discharge is supplied from the Technix SR20-R-1200 power supply, with output voltage 0–20 kV and current 0–60 mA and 1.5 kW input power. The resistor is a standard Tesla  $20 M\Omega \pm 5\%$  type.

This corona probe is then placed into the blown-out plasma jet and analyzed by optical emission spectroscopy (Figs. 1 and 2). Emitted light is guided through the optical bench containing an aperture, a fused silica lens and optical fiber holder. The optical bench is movable horizontally and vertically. Ocean Optics SD2000 spectrometer with two gratings covering the spectral ranges of 200–500 and 500–1100 nm is used. It is very important to get the spectra from the very exact point (the tip of the needle) where the corona discharge is applied. For this reason, the corona needle is placed in the micrometric movable holder, which enables the vertical and horizontal

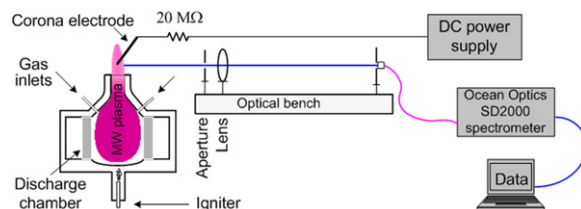


Fig. 1. Experimental set-up. Corona discharge combined with the MW plasma and OES diagnostics.

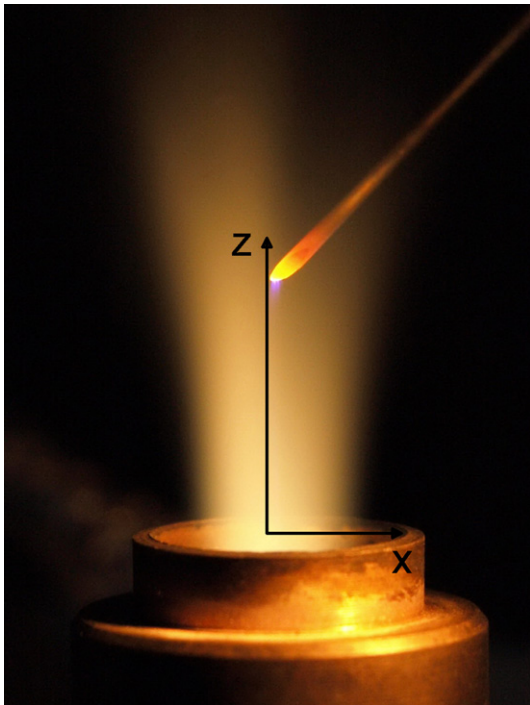


Fig. 2. Corona probe in the MW air plasma.

movement. There was very little thermal degradation of the needle material after a few months of operation with the studied MW torch powers (268–470 W).

#### 4. Results

We applied corona discharge into the MW plasma jet to measure its gas temperature. Both corona and MW plasma were operated in ambient air at atmospheric pressure. The operating pressure was not changed during the experiments. We did not detect any interaction between the corona discharge and microwave plasma jet, the corona discharge did not affect the parameters of the MW plasma (magnetron voltage, current and reflected power were not altered). All MW plasma parameters were continuously measured and the values before and after addition of the corona were identical or within the error range. We performed an experimental test where corona voltage  $U_c$  was changed and no change of the MW plasma parameters was observed. This proved that changing of  $U_c$  did not influence the MW plasma parameters. Vice versa, the MW plasma did not have an influence on the corona discharge—when the gas flow rate  $Q$  and the power  $P$  of MW discharge were changed, corona voltage  $U_c$  and corona current  $I_c$  did not change.

When we applied the corona discharge into the MW plasma, the typical  $U_c$  was 3.52 kV and  $I_c$  was 50  $\mu$ A. This gives the corona power  $P_c=179$  mW, which is negligible compared to the MW plasma powers (hundreds of watts). The energy density in this case was 2.15 J/l. We normally did not change  $U_c$  and  $I_c$  during experiments but we performed one such experiment to test whether changing of  $U_c$  and  $I_c$  changes the measured temperatures of the

MW plasma. For this, we kept the parameters of the MW plasma constant and we only changed  $U_c$  (in the range from 2.56 kV to 3.6 kV, i.e. power  $P_c$  from 57 mW to 180 mW). It had no influence on the measured temperature of the MW plasma jet. The temperature of the MW plasma was also measured by the thermocouple before and after the addition of the corona discharge and it was not changed in any way.

We determined  $T_g$  of the MW plasma as a rotational temperature of  $N_2$  generated in the corona discharge. SPECAIR [16] was used for the spectral simulations that were then fitted to the measured spectra. The typical measured  $N_2$  ( $C^3\Pi_u-B^3\Pi_g$ ) spectrum is shown in Fig. 3.

By this method, we measured the temperature profiles (temperatures at various lateral positions  $x$ , i.e. distances from the vertical plasma axis) of the MW plasma at various conditions—power  $P$  and gas flow rate  $Q$  in various heights  $z$ . The maximum temperature was not found directly in the center of the plasma (at the vertical  $z$ -axis) as expected but it was shifted to the side. This is a result of the plasma shape, which depends on the gas flow conditions. At lower gas flow rates, the generated plasma has a symmetric conical shape and the maximum temperature is usually at (or very close to) the  $z$ -axis, which is the case of  $Q=5$  (normal) l/min (Fig. 4).

With the higher gas flow rates, the shape of the plasma was not symmetric, because plasma was strongly blown out. We would need to increase the power if the conical shape should be maintained but the magnetron power was quite low so in the case of  $Q=8$  or 11 (normal) l/min (Fig. 5) it was not possible to maintain stable conical-shaped plasma. We also measured the vertical temperature profiles (dependence on the height  $z$  above the nozzle). The results show that the temperature is mostly decreasing with  $z$  (Fig. 6).

To test the reliability of the corona probe method we measured the MW plasma  $T_g$  by the corona probe and the thermocouple simultaneously. We used a PeakTech K-type thermocouple for the temperature measurements. It is a chromel–alumel thermocouple (chromel=90% nickel,

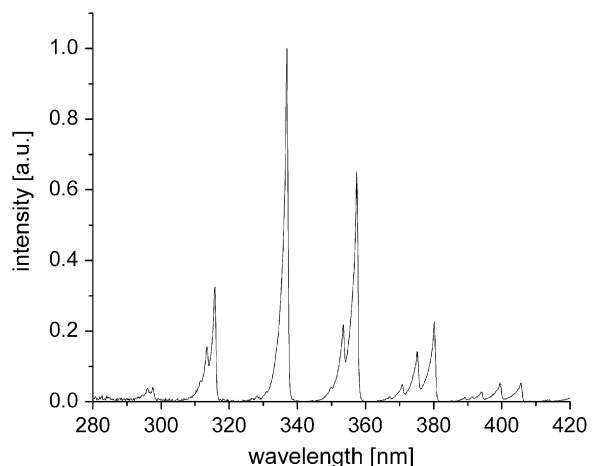


Fig. 3. Typical  $N_2$  second positive spectrum measured by the corona probe in the MW air plasma with properties  $Q=5$  l/min and  $P=368$  W, DC corona 3.5 kV.

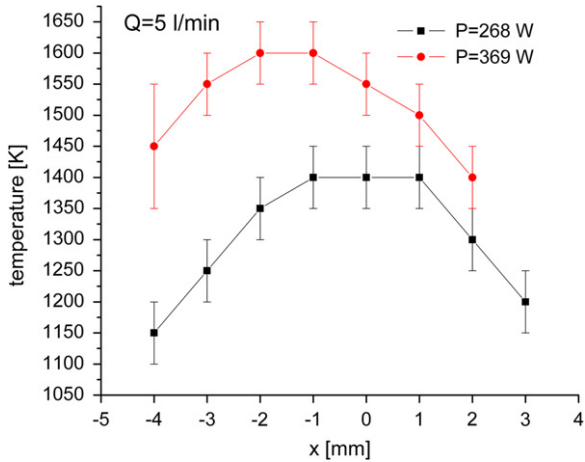


Fig. 4. Dependence of plasma temperature on the lateral position  $x$  in  $z=0$  mm for  $Q=5$  l/min.

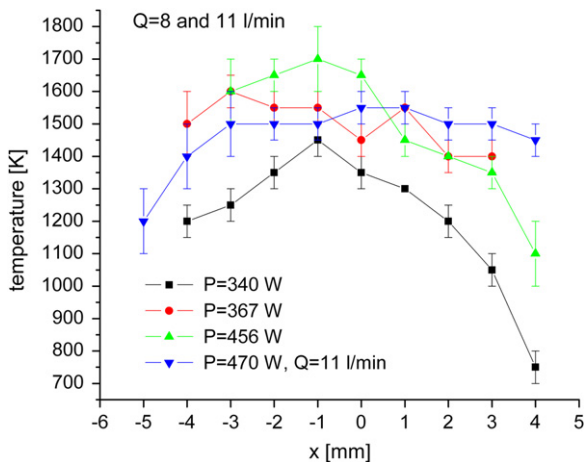


Fig. 5. Dependence of plasma temperature on the lateral position  $x$  in  $z=0$  mm for  $Q=8$  and 11 l/min.

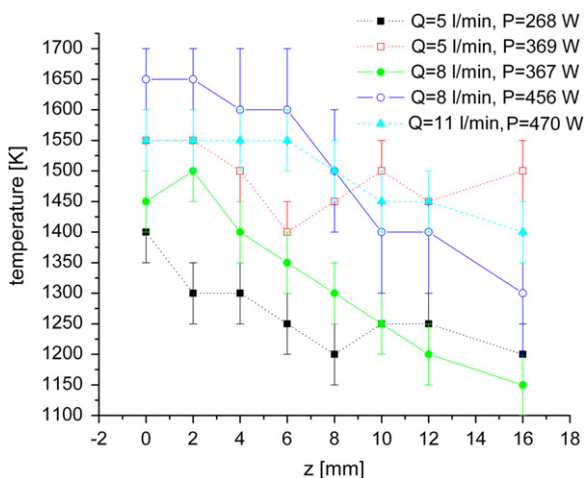


Fig. 6. Dependence of plasma temperature on the height  $z$  in  $x=0$  mm at various operating conditions ( $P$ ,  $Q$ ).

10% chromium and alumel=95% nickel, 2% aluminum and other components) with the temperature range 0–1000 °C. The K-type thermocouple and the corona electrode were placed at the same movable holder and the holder was shifted during the measurement in such a way that either the corona electrode or the thermocouple was in the desired measuring position. The time delay between the corona probe and the thermocouple measurement was only a few seconds (until the holder was moved from one position to another). During this time, the parameters of the MW plasma did not change. These experiments were done at two various gas flow rates  $Q=5$  and 8 l/min and a constant MW power  $P=367$  W. We measured the temperature profiles of the MW plasma in the height  $z=16$  mm above the nozzle because it enabled us to measure the whole temperature profile. In the positions  $z < 16$  mm, the temperature (in the middle of the plasma, at  $x=0$  mm) was above the thermocouple's measuring range (max ~1300 K). On the other hand, in the positions  $z > 16$  mm, the  $N_2$  emission was quite weak, especially at the sides of the plasma. The maximum temperature for  $Q=5$  l/min measured by the corona probe was  $1450 \pm 50$  K and by the thermocouple  $1350 \pm 20$  K (Fig. 7). For  $Q=8$  l/min, the maximum temperature measured by the corona probe was  $1180 \pm 50$  K and by the thermocouple  $1090 \pm 10$  K (Fig. 8). The results show that the temperatures measured by the corona method were slightly higher (up to 150 K) than the thermocouple temperature, but the difference is small relative to the measured plasma temperatures ( $T_g$  close to or above 1000 K).

However, the thermocouple temperature measurements may be affected by radiative losses. So we tried to correct the measured temperatures for these radiative losses. We developed an experimental method based on the measurements of the temporal thermocouple temperature increase coupled with the theoretical assumptions of heat transfer and radiation. This method is described in Appendix A. It is known that the radiative

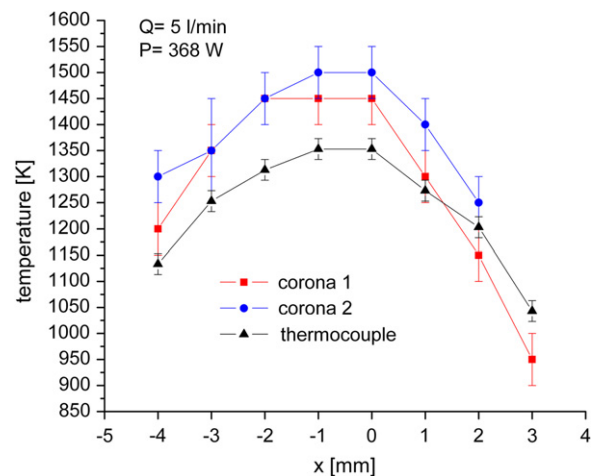
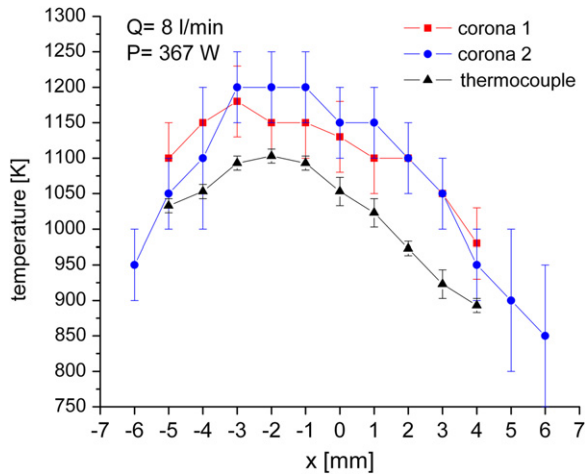


Fig. 7. Comparison of the  $T_g$  temperatures measured by the corona probe and the thermocouple at air flow 5 l/min and MW power 368 W,  $z=16$  mm. Corona 1 and 2 were two sets of measurements.



**Fig. 8.** Comparison of the  $T_g$  temperatures measured by the corona probe and the thermocouple at air flow 8 l/min and MW power 367 W,  $z=16$  mm. Corona 1 and 2 were two sets of measurements.

**Table 1**

The comparison of the temperatures measured by two thermocouples with different bead diameters (directly measured and with radiation correction) in the preheated air.

| Position $x$ (mm) | $T$ measured (K) |              | $T$ with correction (K) |              |
|-------------------|------------------|--------------|-------------------------|--------------|
|                   | Small bead       | Big bead     | Small bead              | Big bead     |
| -3                | $651 \pm 10$     | $649 \pm 10$ | $704 \pm 35$            | $756 \pm 60$ |
| -2                | $657 \pm 10$     | $649 \pm 10$ | $704 \pm 25$            | $677 \pm 22$ |
| -1                | $648 \pm 10$     | $632 \pm 10$ | $693 \pm 27$            | $682 \pm 37$ |
| 0                 | $664 \pm 10$     | $649 \pm 10$ | $689 \pm 20$            | $672 \pm 14$ |
| 1                 | $660 \pm 10$     | $645 \pm 10$ | $676 \pm 14$            | $665 \pm 20$ |

losses increase with the diameter of the thermocouple bead. Therefore we first measured the temperatures of the preheated air with the two thermocouples of different bead diameters (1.5 and 1 mm). An ohmic flow heater (hot air gun) was used to preheat the air flow in this case. The temperatures were measured in various horizontal positions  $x$  of the preheated air outflow in the height approximately 2 cm above the heater exit.

The measured temperatures (without the correction) with the smaller bead were slightly higher than with the bigger bead (Table 1). After the radiative loss correction, the two temperatures agreed within the uncertainty limits resulting from the correction method.

Since the smaller bead thermocouple is less susceptible for radiative losses, we decided to use this one for further measurements. In the next step, we compared the temperatures of the air preheated by the ohmic flow heater measured by the corona probe and the (small bead) thermocouple (without and with the radiation correction). As shown in Fig. 9, the thermocouple directly measured temperatures that are again below the corona probe temperatures. After the correction, the thermocouple temperatures have increased. Compared to the corona temperatures they are just slightly higher but the difference is still within the error range of the corona measurements.

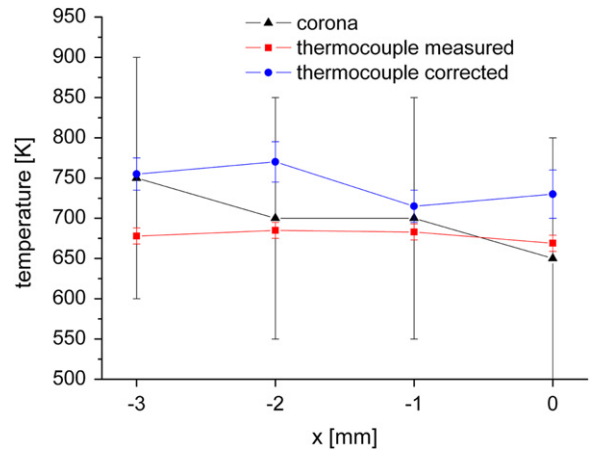


**Fig. 9.** Comparison of the temperatures of the air flow preheated by ohmic heater measured by the corona probe and the thermocouple (with and without correction).

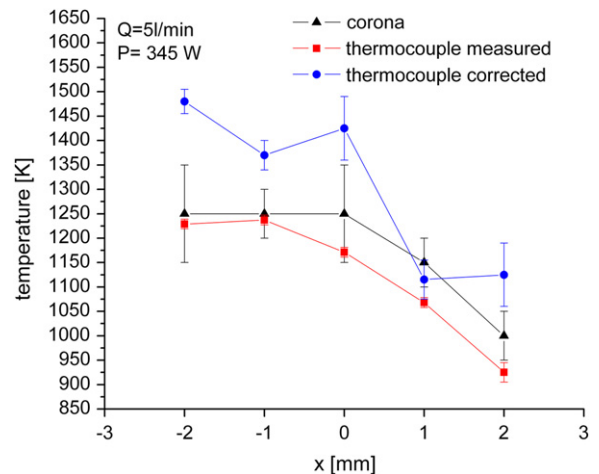


**Fig. 10.** Comparison of the gas temperatures measured by the corona probe and the thermocouple (with and without correction) at air flow 5 l/min and MW power 345 W.

Finally we used the thermocouple with the small bead (without and with the correction for radiative losses) to measure the temperatures of the MW plasma jet and we compared them with the corona probe. The results are shown in Fig. 10. Again, the measured thermocouple temperatures were below corona temperatures. The correction for radiative losses increased these temperatures. In this case, the corrected thermocouple temperatures are mostly higher than the corona temperatures. This may be due to the interaction of the thermocouple bead and connecting wires with the spatially variable electromagnetic field around the MW torch and/or due to the heat conduction from the thermocouple bead through the wires. This interesting phenomenon should be further studied in future. Besides radiative losses that have to be properly corrected for, this indicates another drawback of the thermocouple use for MW plasma temperature measurements.

## 5. Conclusions

We developed and tested a diagnostics method of temperature measurements of near-LTE MW air plasma. A strongly non-equilibrium corona discharge applied inside the atmospheric pressure MW air plasma jet is used as an excitation source for  $N_2^*$  suitable for OES diagnostics. The lateral and axial gas temperature profiles of the MW plasma jet were measured at various powers and flow rates. The comparison of the temperatures measured by this method and by the thermocouple showed that the temperatures measured by the corona probe were slightly higher. This is because thermocouple radiative losses have to be taken into account. After the correction for these losses, temperatures measured by the thermocouple and the corona probe showed a better agreement. Nevertheless, we demonstrated that the corona probe method has several advantages compared to the use of thermocouples:

- it can be applied to high temperature plasmas, out of the typical range of thermocouple use,
- it is not affected by the radiative losses,
- it is not vulnerable to the interaction with the MW plasma or associated electromagnetic fields and/or to the heat conduction through the connecting wires.

In summary, the presented non-equilibrium corona discharge temperature probe, unlike thermocouples, can be considered a reliable method for the near-equilibrium plasma temperature determination, even for plasma with no radiation applicable for spectroscopic temperature measurement.

## Acknowledgments

Effort sponsored by the AFOSR, Air Force Material Command, USAF, under Grant FA8655-09-1-3110, and Slovak Research and Development Agency APVV SK-FR-0038-09 and Comenius University grant UK/368/2011. We gratefully acknowledge Sencera, Ltd. for providing the MW torch.

## Appendix A

*Dynamic temperature measurement by a thermocouple: correction for radiative losses*

*Used symbols*

|       |  |
|-------|--|
| $c$   | specific heat of the thermocouple material [J/kg K]  |
| $h$   | coefficient of the heat transfer from the gas to the thermocouple surface [W/m <sup>2</sup> K] |
| $S$   | effective thermocouple bead surface [m <sup>2</sup> ]  |
| $t$   | time [s]   |
| $T$   | temperature of the thermocouple [K]  |
| $T_g$ | gas temperature [K]  |
| $T_0$ | ambient temperature (initial temperature) [K]  |
| $T_u$ | steady-state temperature [K]   |

|               |  |
|---------------|--|
| $V$           | effective volume of the heated part of the thermocouple (bead) [m <sup>3</sup> ] |
| $\varepsilon$ | emissivity of the thermocouple surface   |
| $\rho$        | specific mass (density) of the thermocouple material [kg/m <sup>3</sup> ]        |
| $\sigma$      | Stefan–Boltzmann constant [W/m <sup>2</sup> K <sup>4</sup> ]                     |

*Equations of temporal evolution of thermocouple temperature*

The thermocouple heating is described by this equation, if heat conduction by the two connecting wires is neglected:

$$\rho c V \frac{dT}{dt} = hS(T_g - T) - \varepsilon \sigma S(T^4 - T_0^4) \quad (1)$$

The first term on the right side represents the thermocouple heating by the heat transfer from the hot gas. The second term represents the radiative losses. For simplicity, let us introduce the following constants:

$$A = \frac{hS}{\rho c V}; \quad B = \frac{\varepsilon \sigma S}{\rho c V}$$

Then we get

$$\frac{dT}{dt} = A(T_g - T) - B(T^4 - T_0^4) \quad (2)$$

In the limit case  $t \rightarrow \infty$ , the thermocouple temperature will reach a steady-state value  $T_u$  and the time derivative of  $T$  becomes 0. Eq. (2) then gets this form

$$0 = A(T_g - T_u) - B(T_u^4 - T_0^4) \quad (3)$$

From this equation we can get the corrected gas temperature  $T_g$

$$T_g = T_u + \frac{B}{A}(T_u^4 - T_0^4) \quad (4)$$

If constants A and B are known and we subtract Eq. (3) from Eq. (2) we get

$$\frac{dT}{dt} = A(T_u - T) + B(T_u^4 - T^4) = (T_u - T)[A + B(T_u + T)(T_u^2 + T^2)] \quad (5)$$

or

$$\frac{1}{T_u - T} \frac{dT}{dt} = A + B(T_u + T)(T_u^2 + T^2) \quad (6)$$

If in time  $t=0$  we insert the thermocouple into the hot gas flow with the temperature  $T_g$ , then  $T=T_0$ . Then we get by integration in time from 0 to  $t$

$$-[\ln(T_u - T)]_{T_0}^T = At + B \int_0^t (T_u + T(x))(T_u^2 + T^2(x)) dx \quad (7)$$

or

$$-\frac{1}{t} \ln \frac{T_u - T(t)}{T_u - T_0} = A + B \frac{1}{t} \int_0^t (T_u + T(x))(T_u^2 + T^2(x)) dx \quad (8)$$

Let us designate the limit for  $t \rightarrow 0$  ( $T(t) \rightarrow T_0$ ) as  $K$

$$K = -\lim_{t \rightarrow 0} \frac{1}{t} \ln \frac{T_u - T(t)}{T_u - T_0} \quad (9)$$

This  $K$  represents the slope of the tangent line of the function  $T(t)$  for  $t=0$ . For  $t \rightarrow 0$  we get from Eq. (8)

$$A = K - B(T_u + T_0)(T_u^2 + T_0^2) \quad (10)$$

Finally, by eliminating  $A$  in (8) we get

$$-\frac{1}{t} \ln \frac{T_u - T(t)}{T_u - T_0} = K + B \frac{1}{t} \int_0^t [(T_u + T(x))(T_u^2 + T^2(x)) - (T_u + T_0)(T_u^2 + T_0^2)] dx \quad (11)$$

And we get the final result

$$-\frac{1}{t} \ln \frac{T_u - T(t)}{T_u - T_0} = K + B \frac{1}{t} J(t) \quad (12)$$

where

$$J(t) = \int_0^t (T(x) - T_0)[T^2(x) + (T_u + T_0)(T(x) + T_0) + T_u^2] dx \quad (13)$$

*Application of the theory to the hot gas temperature measurements*

We employ the temporal evolution of the thermocouple temperature increase  $T(t)$  measured by the 100 MHz digitizing oscilloscope Rigol DS1102E. The integral function  $J(t)$  was determined by successive additions of the values in the integrand for temperatures  $T(t)$  stored by the oscilloscope

$$J(t_n) \approx \sum_{i=1}^n (T(x_i) - T_0)[T^2(x_i) + (T_u + T_0)(T(x_i) + T_0) + T_u^2] \delta x \quad (14)$$

where  $n$  is the number in the data file,  $\delta x$  is the temporal step and  $t_n = n \delta x$ .

To obtain the radiative losses correction we first determine the constants  $B$  and  $K$  from Eq. (12). By iterations we seek  $B$ , where the expression

$$-\frac{1}{t} \left[ \ln \frac{T_u - T(t)}{T_u - T_0} + B J(t) \right] = K \quad (15)$$

is constant for the measured  $T(t_n)$  and  $J(t_n)$ . It is advantageous to display the result in a graph as a function of  $T(t_n)$  instead of time.

From Eq. (12) we calculate the temperature  $T$

$$T(t) = T_u - (T_u - T_0)e^{-[Kt + B J(t)]} \quad (16)$$

and then by changing the constants  $K$  and  $B$  we fit the temperature  $T$  onto the measured temporal evolution. After knowing  $K$  and  $B$  we can calculate the gas temperature  $T_g$  from Eqs. (10) and (4).

Finally we show the example results of the application of this theory to determine the gas temperature of the hot air gun. Fig. A1 shows the thermocouple heating from the initial temperature  $T_0 = 305.3$  K to the steady-state temperature  $T_u = 633.8$  K.

Fig. A2 shows the function (16) approximating the measured data for  $K = 0.69$  and  $B = 0$ . The best fit was in this case obtained for  $B = 1.92 \times 10^{-10}$  (Fig. A3). Bezier curves were used in the graph in Fig. A2. After knowing the constants  $K$  and  $B$ , we use Eqs. (4) and (10) to calculate the corrected gas temperature  $T_g = 683$  K.

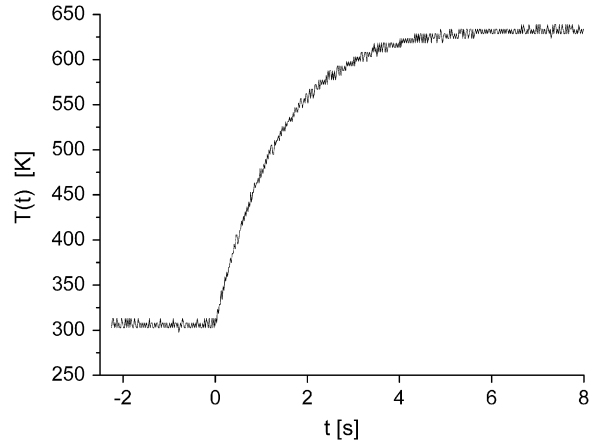


Fig. A1. Temporal evolution of the thermocouple temperature after inserting into the gas flow of the hot air gun.

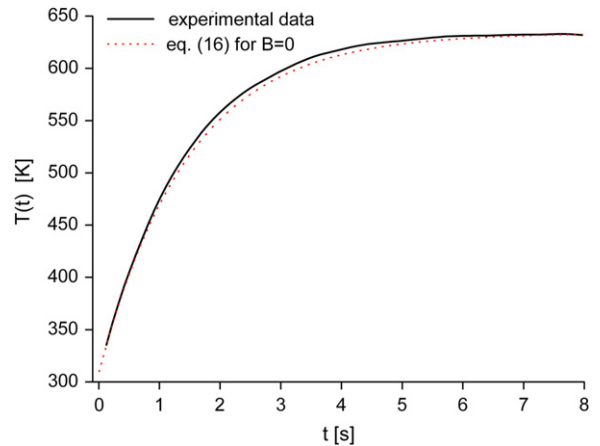


Fig. A2. Comparison of the Eq. (16) with measured  $T(t)$  for  $K = 0.69$  and  $B = 0$ .

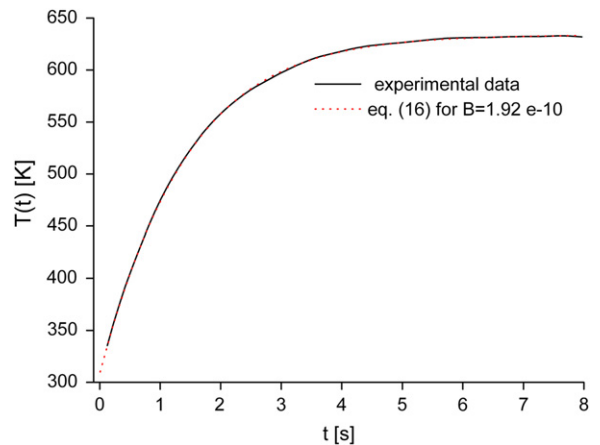


Fig. A3. Test of the Eq. (16) with experiment for  $K = 0.69$  and  $B = 1.92 \times 10^{-10}$ .

## References

- [1] Al-Shamma'a AI, Wylie SR, Lucas J, Pau CF. Design and construction of a 2.45 GHz waveguide-based microwave plasma jet at atmospheric pressure for material processing. *Journal of Physics D: Applied Physics* 2001;34:2734–41.
- [2] Uhm HS, Hong YC, Shin DH. A microwave plasma torch and its applications. *Plasma Sources Science and Technology* 2006;15: S26–34.
- [3] Zajickova L, Elias M, Jasek O, Kudrle V, Frgala Z, Matejkova J, et al. Atmospheric pressure microwave torch for synthesis of carbon nanotubes. *Plasma Physics and Controlled Fusion* 2005;47: B655–66.
- [4] Green KM, Borrás MC, Woskov PP. Electronic excitation temperature profiles in air microwave plasma torch. *IEEE Transactions on Plasma Science* 2001;29:399.
- [5] Lee MH, et al. Removal and sterilization of biofilms and planktonic bacteria by microwave-induced argon plasma at atmospheric pressure. *New Journal of Physics* 2009;11:115022.
- [6] Weltmann K-D, Brandenburg R, von Woedtke T, Ehlbeck J, Foest R, Stieber M, et al. Antimicrobial treatment of heat sensitive products by miniaturized atmospheric pressure plasma jets (APPJs). *Journal of Physics D: Applied Physics* 2008;41(194008):6.
- [7] Yu L, Laux CO, Packan DM, Kruger CH. Direct-current glow discharges in atmospheric pressure air plasmas. *Journal of Applied Physics* 2002;91:2678–86.
- [8] Pai DZ, Lacoste DA, Laux CO. Transitions between corona, glow, and spark regimes of nanosecond repetitively pulsed discharges in air at atmospheric pressure. *Journal of Applied Physics* 2010;107:093303.
- [9] Fantz U. Basics of plasma spectroscopy. *Plasma Sources Science and Technology* 2006;15:S137–47.
- [10] Machala Z, Janda M, Hensel K, Jedlovský I, Leštinská L, Foltin V, et al. Emission spectroscopy of atmospheric pressure plasmas for biomedical and environmental applications. *Journal of Molecular Spectroscopy* 2007;243:194–201.
- [11] Laux CO, Spence TG, Kruger CH, Zare RN. Optical diagnostics of atmospheric pressure air plasmas. *Plasma Sources Science and Technology* 2003;12:125–38.
- [12] Moon SY, Choe W, Uhm HS, Hwang YS, Choi JJ. Characteristics of an atmospheric microwave-induced plasma generated in ambient air by an argon discharge excited in an open-ended dielectric discharge tube. *Physics of Plasmas* 2002;9:4045.
- [13] Anghel SD, Simon A. An alternative source for generating atmospheric pressure non-thermal plasmas. *Plasma Sources Science and Technology* 2007;16:B1–4.
- [14] Meng X, Pan WX, Chen X, Wu CK. Measured temperature of a laminar plasma jet by using thermocouple at reduced pressure. In: *Proceedings of the 19th International Symposium on Plasma Chemistry*, Bochum; July 26–31 2009.
- [15] Foltin V, Leštinská L, Machala Z. Spectroscopic investigations of atmospheric pressure microwave torch nitrogen plasma jet. *Czechoslovak Journal of Physics* 2006;56:B712–720.
- [16] Laux CO. Radiation and nonequilibrium collisional-radiative models. In: Fletcher D, Magin T, Charbonnier J-M, Sarma GSR, editors. *Physico-chemical modeling of high enthalpy and plasma flows*. von Karman Institute for Fluid Dynamics. Lecture Series 2002–07. Rhode Saint-Genese, Belgium; June 4–7 2002 <www.specair-radiation.net>.